Tissue structure accelerates evolution: premalignant sweeps precede neutral expansion

Jeffrey West[1,*], Ryan O. Schenck[1,2], Chandler Gatenbee[1], Mark Robertson-Tessi[1], and Alexander R. A. Anderson[1,+]

[1]Integrated Mathematical Oncology Department, H. Lee Moffitt Cancer Center & Research Institute, 12902 Magnolia Drive, SRB 4 Rm 24000H Tampa, Florida, 33612
[2]Wellcome Centre for Human Genetics, University of Oxford, Oxford, OX37BN, UK
[*]jeffrey.west@moffitt.org
[+]Alexander.Anderson@moffitt.org

Cancer has been hypothesized to be a caricature of the renewal process of the tissue of origin: arising from (and maintained by) small subpopulations capable of continuous growth[1]. The strong influence of the tissue structure has been convincingly demonstrated in intestinal cancers where adenomas grow by the fission of stem-cell-maintained glands influenced by early expression of abnormal cell mobility in cancer progenitors[2,3]. So-called "born to be bad" tumors arise from progenitors which may already possess the necessary driver mutations for malignancy[4,5] and metastasis[6]. These tumors subsequently evolve neutrally, thereby maximizing intratumoral heterogeneity and increasing the probability of therapeutic resistance. These findings have been nuanced by the advent of multi-region sequencing, which uses spatial and temporal patterns of genetic variation among competing tumor cell populations to shed light on the mode of tumor evolution (neutral or Darwinian) and also the tempo[4,7–11]. Using a classic, well-studied model of tumor evolution (a passenger-driver mutation model[12–16]) we systematically alter spatial constraints and cell mixing rates to show how tissue structure influences functional (driver) mutations and genetic heterogeneity over time. This model approach explores a key mechanism behind both inter-patient and intratumoral tumor heterogeneity: competition for space. Initial spatial constraints determine the emergent mode of evolution (neutral to Darwinian) without a change in cell-specific mutation rate or fitness effects. Transition from early Darwinian to late neutral evolution is accelerated by the combination of two factors: spatial constraints and well-timed dispersal events.

Cancer is characterized by tens of thousands of somatic alterations, which may be classified into drivers (conferring advantageous, cancerous phenotypes to neoplastic cells) and passengers (neutral, nearly-neutral, or slightly deleterious mutations). Highly deleterious mutations are subject to negative selection and are removed from the population, while moderately deleterious mutations can evade purifying selection to remain present in an evolving tumor under selection pressure, a process known as "hitchhiking" with the sweeping driver clone[15,17].

Patterns of intratumoral genetic heterogeneity (ITH) and subclonal architecture are the direct consequence of the evolutionary dynamics of tumor growth. Multiregion sequencing has produced evidence that Darwinian evolution shapes at least part of ITH[10,18]. Substantial increases in subclone fitness have been observed in some cases: 21% of colon cancers, 29% of gastric cancers, and 53% of metastases[5]. Tumorigenesis primarily favors selective sweeps since early tumor growth must deal with obstacles such as spatial constraints, nutritional limitation, and immune attack[11]. However, the parental clone that can conquer these obstacles emerges from the subclones generated by early Darwinian evolution. This evolutionary bottleneck establishes the driver mutations in the parental, invasive clone as ubiquitous mutations in a neutral evolutionary phase of tumor growth, after invasion[11,19].

How does tissue structure influence somatic evolution? Some have speculated that modes of evolution (Darwinian to neutral) may be the outcome of cellular architecture of the tumor (e.g. the glandular structure of colorectal cancers limits the effects of selection), or of the malignancy's anatomical location, governing access to resources or strong spatial constraints for growth[5,20]. Some structures are "amplifiers" of natural selection, improving the odds of advantageous mutants[21] (e.g. pancreatic ducts that control migration rates between patches[22] and spatially segregated colon glands with a centralized stem cell pool[3]). The well-defined tissue structure begins to break down as the cancer transitions to increasing invasiveness, often with sudden, "punctuated" accrual of copy number alterations needed to facilitate invasion into the stroma[23,24]. It is our point of view that this switch from Darwinian to neutral evolution is highly influenced by the tissue structure where the founding clone arises.

Functional and genetic heterogeneity

While many mathematical passenger-driver tumor evolution models use branching processes[25] or stochastic, well-mixed (non-spatial), agent-based models[12,13,26], some have investigated the role of *spatial* competition on local heterogeneity and

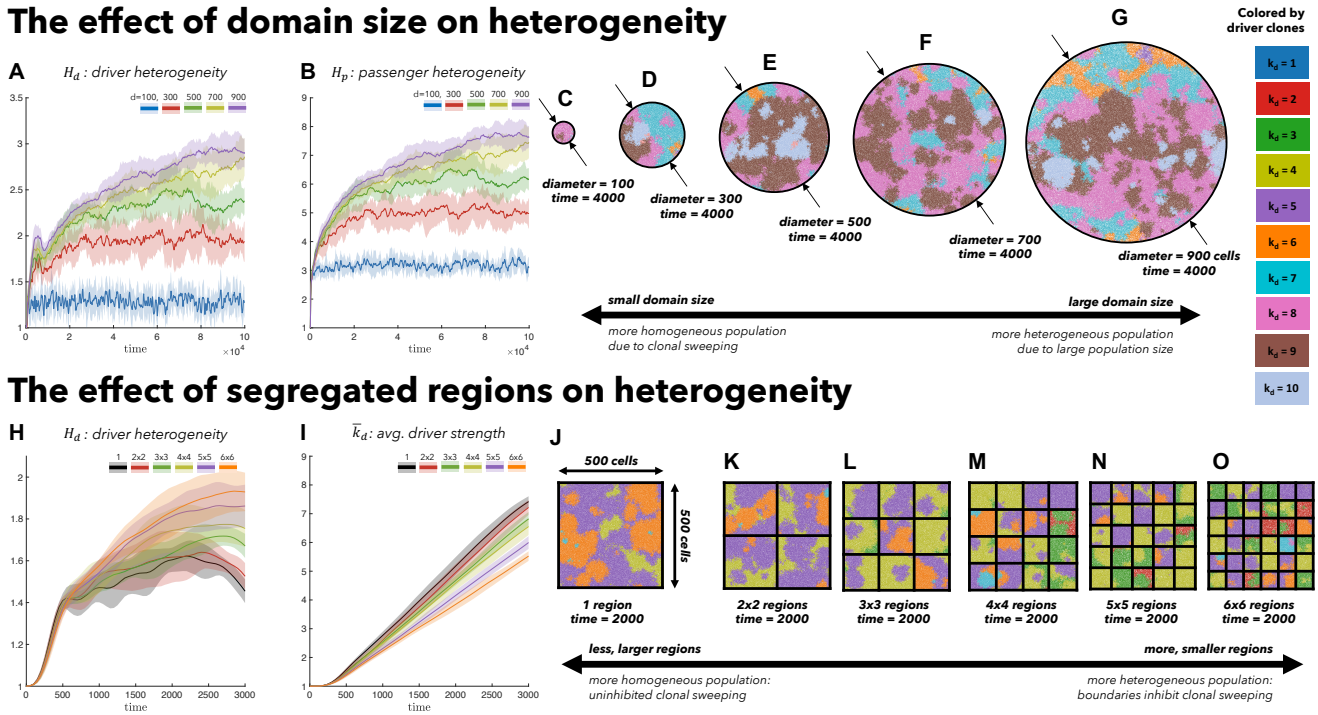

Figure 1. The effect of spatial constraints on heterogeneity: Cells divide and die on a regular square lattice. A cell selected for birth can divide only into an empty grid location and may accrue passenger or driver mutations. Top: simulations on varied sizes of domains, ranging from 100 cells in diameter to 900 cells, seeded with 100 cells ($k_d = 1.$ $k_p = 0$) at time zero ($T_p = 5 \cdot 10^6$,$T_d = 700$,$s_d = 0.1$, $s_p = 0.01$). (A,B) An increase in domain size results in increased driver and passenger heterogeneity, with standard deviation shown (shaded colors) for 10 stochastic simulations. (C,D,E,F,G) Representative snapshots after 4000 cell generations. Bottom: Identical domain size (seeded with one-third of the domain filled; $k_d = 1.$ $k_p = 0$) segregated into varied number of non-interacting regions ($T_p = 10^6$, $T_d = 700$, $s_d = 0.1$, $s_p = 0.01$, $\mu = 10^{-8}$). (H) driver heterogeneity increases with number of segregated regions. (I) Boundaries limit new clones from expanding beyond a single region, decreasing the average number of drivers in the population. (J,K,L,M,N,O) Representative snapshots after 2000 cell generations. See attached video S3.

circulating tumor cells[16], resistance to therapy[27], metastasis[6,14], and trade-offs between migration and proliferation[28]. The model introduced here is a spatially-explicit extension of a previously published non-spatial model of passengers and drivers in tumor evolution[12,13,15]. Tumor evolution is played out on a two- or three-dimensional grid where each grid point can contain at most one cell. Each cell carries heritable genetic changes classified into driver mutations (e.g. an activating mutation in KRAS) or passenger mutations. Cells begin each simulation with a single driver mutation, where each subsequent driver increases the birth rate (i.e. multiplicative epistasis) by a factor of a fitness advantage parameter, s_d. Similarly, passenger mutations decrease the birth rate by a factor of fitness penalty, s_p (see figures S1 and S2).

Tumors constrained to smaller domain sizes (figure 1, top; video S3, top) show consistently lower driver and passenger diversity than for larger domain sizes. Small, tightly-coupled homogeneous populations of cells are able to quickly sweep each successive driver mutation. Larger domains consist of a heterogeneous population; with many more cell divisions, the odds of accruing another driver mutation are increased, but they have little chance of sweeping through the large domain.

To control for population size effects in this evolutionary arms race, identical domains are segregated into non-interacting regions of varying size (figure 1, bottom). Again, smaller (highly constrained) regions provide a stronger selection force, sweeping away weaker subclones. This sweeping stops at each region's boundaries, resulting in a heterogeneous population of locally homogeneous regions (figure 1H). Boundaries limit new clones from expanding beyond a single region, decreasing the average number of drivers in the population (figure 1I).

Modeling the acceleration of evolution by tissue structure

Bounded, non-interacting regions play a role in human cancers, which are often locally constrained to a single gland or a duct. Such glandular or ductal structures allow for limited cellular dispersal or mixing during premalignant growth, enabling the tumor to explore new (and often less constrained) environments. In figure 2, each segregated region may now circulate cells into a neighboring region at a low or high rate of dispersal (left and right columns, respectively). Tumors evolve on two axes: genetic (mutation burden; x-axis) and phenotypic (average number of driver mutations, $\bar{k}_d$; y-axis). The evolution of an

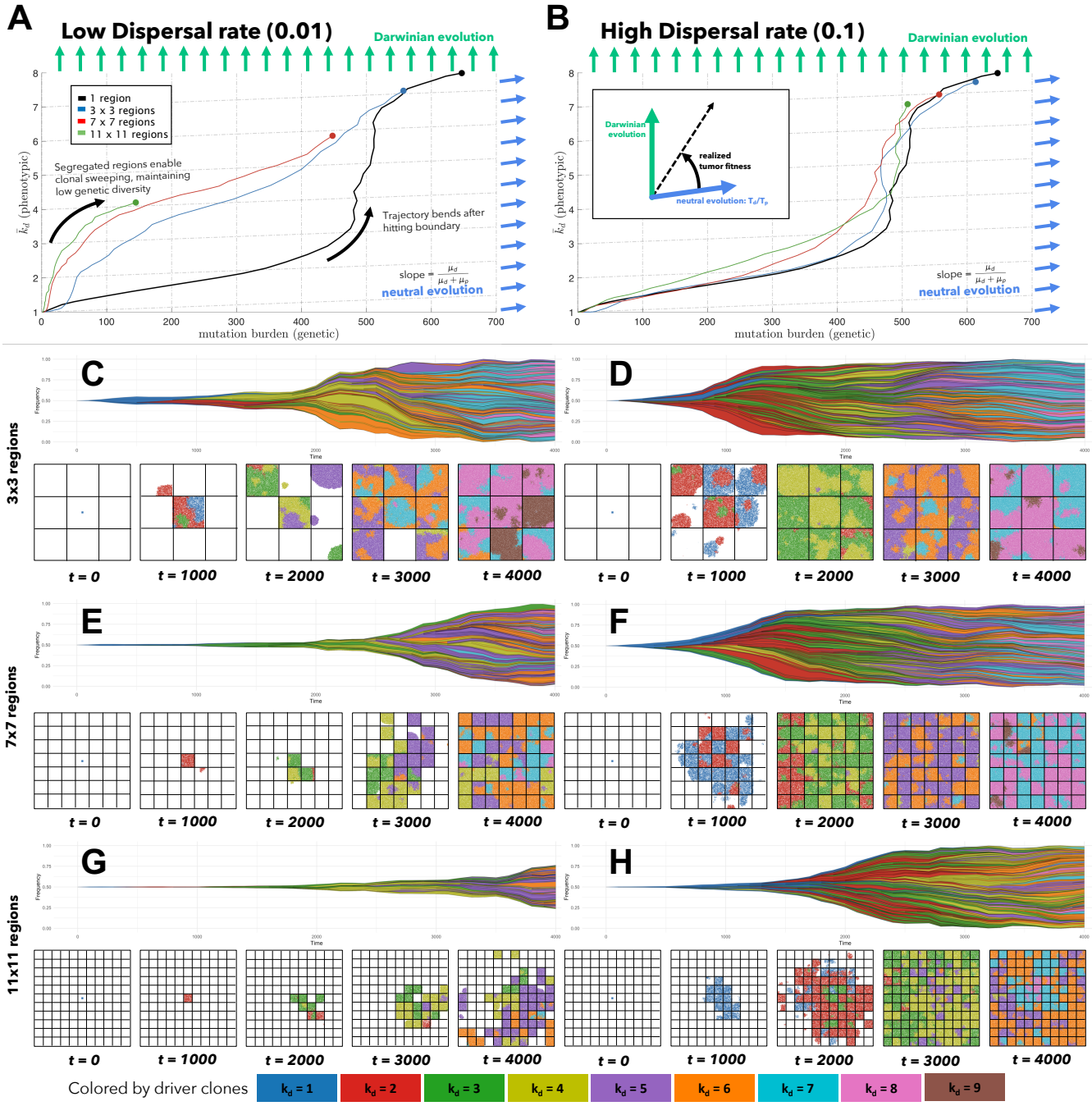

Figure 2. Spatial segregation with cell dispersal accelerates evolution: (A,B) Tumors evolve on the genetic (mutation burden; x-axis) and phenotypic (average drivers; y-axis) axes over 4000 cell generations. Simulations seeded with 100 cells ($k_d = 1$, $k_p = 0$) are allowed to disperse between segregated regions at a low rate (0.01; left column) or high rate (0.1; right column) for varied number of segregated regions (line color). As dispersal increases, tumor evolution "collapses" back onto the unsegregated single region case shown in black in B. (C,D) A Muller plot of tumor evolution represents genotypes color-coded by driver (k_d) value. The horizontal axis is time (cell generations), with height corresponding to genotype frequency. Descendant genotypes are shown emerging from inside their parents. Snapshots shown every 1000 cell generations. Simulations repeated for 7 by 7 regions (E,F), and 11 by 11 regions (G,H). Parameters: $T_p = 5 \cdot 10^6$, $T_d = 700$, $s_d = 0.1$, $s_p = 10^{-3}$, $\mu = 10^{-8}$. See attached video S4.

unsegregated tumor in is shown in black (figure 2A,B), accumulating genetic diversity (left-to-right) over time with a slow accumulation of drivers (bottom-to-top). At later times, the tumor grows to carrying capacity (constrained by the domain size), bending the tumor evolution curve upward to increased $\bar{k}_d$.

"Perfectly neutral" tumors ($s_d = 0$) would acquire drivers at a rate equal to the ratio of drivers to all mutations (figure 2, blue arrows). Conversely, "perfectly Darwinian" tumors would sweep each new driver mutation, resulting in a vertical trajectory (figure 2, green arrows). Tumor diversity can be visualized on a Muller plot, displaying each clone's abundance over time, colored by driver mutations (figure 2C - H; video S4).

Tumors with low dispersal rates (figure 2, left column) tend to evolve by a Darwinian mode of evolution: clonal sweeping which maintains a lower genetic diversity. Increasingly smaller regions allows new drivers to more easily sweep within a local region (figure 2A). Introducing segregated regions increases spatial constraints, allowing the tumor to realize increased levels of selection (figure 2B, inset) even without changes in cell-specific fitness. Importantly, this accelerated mode of evolution is lost when the dispersal rate between regions is too high (see figure 2B). The high dispersal rate (right column) recapitulates the evolutionary trajectory of a relatively unconstrained tumor, decreasing the tumor's realized fitness.

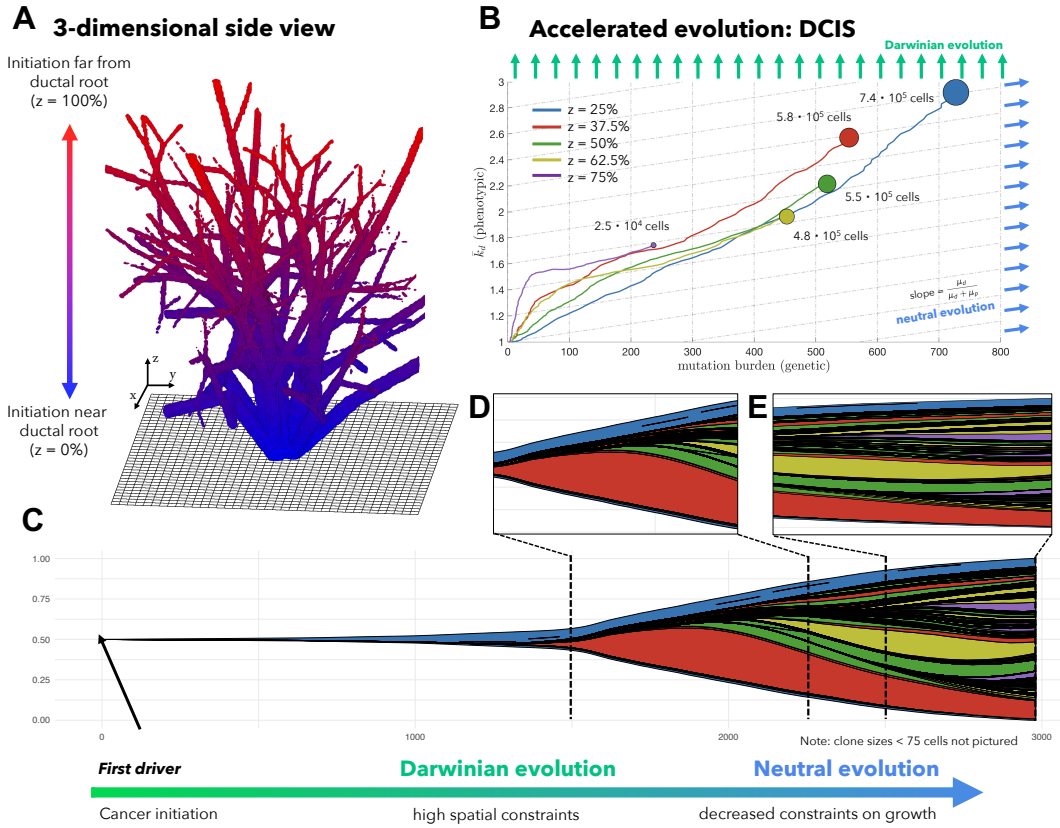

Figure 3. Three dimensional model of tumor evolution constrained by ductal network structure: (A) Realistic three-dimensional topology of breast ductal networks (reconstructed with data from anthropomorphic breast phantoms in[29]) provides full three-dimensional maps to seed and constrain tumor evolution simulations. (B) Tumor evolution is shown for varied initial conditions (z-dimension shown in A; $T_p = 10^6$, $T_d = 700$, $s_d = 0.1$, $s_p = 0.1$, $\mu = 10^{-8}$). Simulations closer to the ductal root (e.g. blue curve) in larger, less constrained branches are characterized by a steady left-to-right (neutral) evolution and constant acquisition of new clones. Simulations further from the ductal root (e.g. purple) in smaller, more constrained branches are characterized by clonal sweeping (bottom-to-top evolution) early, but with a shift toward neutrality (left-to-right) at later times. Each tumor is seeded with 500 cells ($k_d = 1$; $k_p = 0$). Each simulation is run for 3000 cell generations, with final tumor size indicated by size of the circle. A representative Muller plot (normalized by final tumor size) is shown in (C, with insets D,E), where Darwinian evolution with new clones sweeping through the population occurs early in tumor evolution and neutral evolution dominates later (shown for $z = 50\%$). See attached video S5.

Ductal Carcinoma in situ

The branching topology of a breast ductal and glandular network structure acts as a similar evolutionary accelerant, where spatially segregated regions (ductal branches) work in combination with cell dispersal (subject to varied branching topology) to accelerate tumor evolution[30]. In figure 3, the evolution of ductal carcinomas *in situ* is initialized and constrained to grow inside

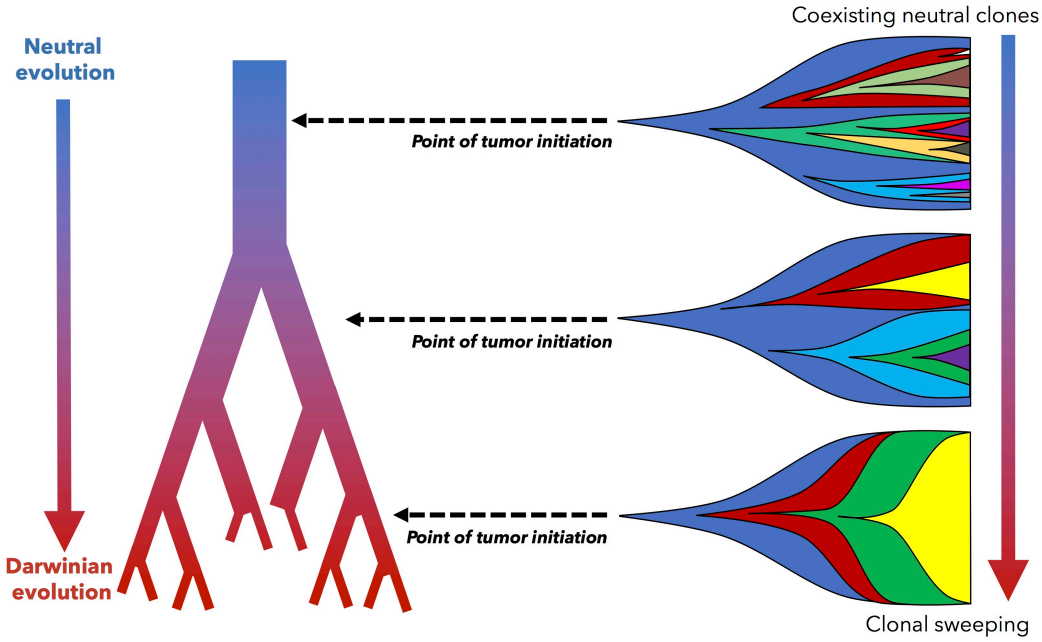

Figure 4. Summary schematic: Simulations near the ductal root in larger, less constrained branches (e.g. top) are characterized by a steady, neutral evolution, consistently acquiring new clones that coexist for extended time periods. A smaller tumor originating in a smaller, more constrained branches far from the ductal root (e.g. bottom) enables an accelerated evolution with clonal sweeping. Levels of selection may be highly heterogeneous between patients, due to the location of tumor initiation.

a ductal network reconstructed with data from anthropomorphic breast phantoms[29]. This provides a realistic three-dimensional topology of a continuously connected series of progressively smaller branches (figure 3A; video S6).

Tumors initiated inside larger ductal branches near the root of the network ($z = 25\%$, blue, figure 3B) begin with less spatial constraints and increased access to expand into new branches. These tumors evolve more neutrally (left-to-right trajectories in figure 3B). Tumors initiated further from the ductal root in smaller, more constrained branches (e.g. purple curve) are characterized by clonal sweeping (vertical trajectories) early. At later times, the tumor expands into new unexplored territories, shifting toward neutral trajectories. Interestingly, the final tumor size (figure 3B, circles) does not necessarily correlate to phenotypic aggressiveness. A tumor originating in a tightly constrained duct enables an accelerated acquisition of drivers and may be a more dangerous, highly homogeneous population of malignant cells which have all acquired new traits such as invasiveness, motility, or metastatic capabilities. While these small tumors may grow more slowly in time, they undergo accelerated phenotypic evolution caused by the strong selection imposed by high spatial constraints.

Surprisingly, two otherwise identical tumors may realize dramatic differences in fitness depending on constraints imposed by tissue architecture. On the cell scale, any given subclone may indeed have a selective advantage (i.e. a higher birth rate). Yet, the effective outcome of this subclonal advantage depends on the surrounding competitive context of that cell. In other words, cell-specific phenotypic behavior can be "overridden" by the tissue architecture, allowing the tumor to realize increased fitness. This approach adds clarity to the debate of neutral tumor evolution by exploring a key mechanism behind both inter-patient and intratumoral tumor heterogeneity: competition for space.

During early tumorigenesis, multiple subclones with unique driver mutations compete according to Darwinian principles of fitness. The tumor is confronted with a growth limitation before progression to late stage, invasive cancer. The parental clone that can conquer this growth limitation was generated by the Darwinian evolution of tumorigenesis. At this point in time, the tumor is effectively under neutral evolutionary dynamics due to a significant loss of selection pressure at the point of invasion. The parental invasive clone undergoes clonal expansion, generating vast intratumoral heterogeneity. Early tumors dominated by Darwinian selection provide a more homogeneous seeding population for metastasis, which unfortunately may be more aggressive.

It is clear that spatial competition can no longer be ignored in evolutionary models of tumor evolution. These results (summarized in figure 4) help to unify the debate surrounding neutral tumor evolution by clarifying the role of space in the transition from Darwinian to neutral evolution. Initial spatial constraints determine the emergent mode of evolution (neutral to Darwinian) without the necessity for changes in cell-specific mutation rate or fitness effects. The branching topology of ductal

networks at tumor initiation determines two important evolutionary accelerants: spatial constraints and cellular dispersal. This connectivity is likely to be highly heterogeneous between patients, leading to variability in rates of cellular dispersal between spatially distinct niches within a tumor. Limited connectivity enables subclones to undergo high levels of local selection due to spatial constraints. These results are generalizable to many solid cancers containing a predictable pattern of spatially distinct regions with a low level of cell mixing like colorectal cancer (glandular fission) and ductal carcinomas (branching topology).

References

1. Pierce, G. B. & Speers, W. C. Tumors as caricatures of the process of tissue renewal: prospects for therapy by directing differentiation. *Cancer Research* **48**, 1996–2004 (1988).
2. Baker, A.-M. *et al.* Quantification of crypt and stem cell evolution in the normal and neoplastic human colon. *Cell Reports* **8**, 940–947 (2014).
3. Ryser, M. D., Min, B.-H., Siegmund, K. D. & Shibata, D. Spatial mutation patterns as markers of early colorectal tumor cell mobility. *Proceedings National Academy Sciences* 201716552 (2018).
4. Sottoriva, A. *et al.* A big bang model of human colorectal tumor growth. *Nature genetics* **47**, 209 (2015).
5. Williams, M. J., Werner, B., Barnes, C. P., Graham, T. A. & Sottoriva, A. Identification of neutral tumor evolution across cancer types. *Nature genetics* **48**, 238 (2016).
6. Reiter, J. G. *et al.* Minimal functional driver gene heterogeneity among untreated metastases. *Science* **361**, 1033–1037 (2018).
7. Jolly, C. & Van Loo, P. Timing somatic events in the evolution of cancer. *Genome biology* **19**, 95 (2018).
8. Swanton, C. Intratumor heterogeneity: evolution through space and time. *Cancer Research* (2012).
9. Gerlinger, M. *et al.* Intratumor heterogeneity and branched evolution revealed by multiregion sequencing. *New England journal medicine* **366**, 883–892 (2012).
10. Caravagna, G. *et al.* Detecting repeated cancer evolution from multi-region tumor sequencing data. *Nature methods* **15**, 707 (2018).
11. Saito, T. *et al.* A temporal shift of the evolutionary principle shaping intratumor heterogeneity in colorectal cancer. *Nature communications* **9**, 2884 (2018).
12. McFarland, C. D., Korolev, K. S., Kryukov, G. V., Sunyaev, S. R. & Mirny, L. A. Impact of deleterious passenger mutations on cancer progression. *Proceedings National Academy Sciences* **110**, 2910–2915 (2013).
13. McFarland, C. D., Mirny, L. A. & Korolev, K. S. Tug-of-war between driver and passenger mutations in cancer and other adaptive processes. *Proceedings National Academy Sciences* **111**, 15138–15143 (2014).
14. Waclaw, B. *et al.* A spatial model predicts that dispersal and cell turnover limit intratumour heterogeneity. *Nature* **525**, 261 (2015).
15. McFarland, C. D. *et al.* The damaging effect of passenger mutations on cancer progression. *Cancer Research* (2017).
16. Ahmed, Z. & Gravel, S. Intratumor heterogeneity and circulating tumor cell clusters. *Molecular biology evolution* (2017).
17. H Heng, H. *et al.* Genetic and epigenetic heterogeneity in cancer: the ultimate challenge for drug therapy. *Current drug targets* **11**, 1304–1316 (2010).
18. Sun, R. *et al.* Between-region genetic divergence reflects the mode and tempo of tumor evolution. *Nature genetics* **49**, 1015 (2017).
19. Uchi, R. *et al.* Integrated multiregional analysis proposing a new model of colorectal cancer evolution. *PLoS genetics* **12**, e1005778 (2016).
20. Williams, M. J. *et al.* Quantification of subclonal selection in cancer from bulk sequencing data. *Nature genetics* 1 (2018).
21. Pavlogiannis, A., Tkadlec, J., Chatterjee, K. & Nowak, M. A. Construction of arbitrarily strong amplifiers of natural selection using evolutionary graph theory. *Communications Biology* **1**, 71 (2018).
22. Makohon-Moore, A. P. *et al.* Precancerous neoplastic cells can move through the pancreatic ductal system. *Nature* 1 (2018).
23. Baker, A.-M. *et al.* Evolutionary history of human colitis-associated colorectal cancer. *Gut* gutjnl–2018 (2018).
24. de Bruin, E. C. *et al.* Spatial and temporal diversity in genomic instability processes defines lung cancer evolution. *Science* **346**, 251–256 (2014).
25. Bozic, I. *et al.* Accumulation of driver and passenger mutations during tumor progression. *Proceedings National Academy Sciences* **107**, 18545–18550 (2010).
26. Wodarz, D., Newell, A. C. & Komarova, N. L. Passenger mutations can accelerate tumour suppressor gene inactivation in cancer evolution. *Journal The Royal Society Interface* **15**, 20170967 (2018).

27. Bacevic, K. *et al.* Spatial competition constrains resistance to targeted cancer therapy. *Nature communications* **8**, 1995 (2017).

28. Gallaher, J., Brown, J. & Anderson, A. R. The dynamic tumor ecosystem: how cell turnover and trade-offs affect cancer evolution. *bioRxiv* 270900 (2018).

29. Jeon, H. *et al.* Generation of polychromatic projection for dedicated breast computed tomography simulation using anthropomorphic numerical phantom. *PloS one* **12**, e0187242 (2017).

30. Macklin, P. & Edgerton, M. E. Patient-calibrated agent-based modelling of ductal carcinoma in situ (dcis) i: Model formulation and analysis. .

31. Bravo, R. R. *et al.* Hybrid automata library: A modular platform for efficient hybrid modeling with real-time visualization. *bioRxiv* 411538 (2018).

Methods

Consistent with previously models of passenger driver evolution, tumors will undergo progression with a low mutation rate (less total deleterious passengers) or a low passenger fitness s_p (see figure S1A,B). We specifically are focused on measures of functional (drivers) and non-functional (passengers) heterogeneity and the conclusions drawn from the model apply in the assumption of neutral or non-neutral passengers.

Code Availability

All figures were produced using an agent-based modeling platform (Java) known as HAL: Hybrid Automata Library[31] (available at: https://github.com/torococo/HAL).

Model Overview

Each model simulation is carried out on a two- or three-dimensional grid lattice where each tumor cell is allowed to occupy a single grid point. Simulations are started with r_0^2 initial cells ($r_0 = 10$ unless otherwise noted). During each time step, each cell undergoes a birth-death process with the following birth (P_b) and death (P_d) probabilities:

$$P_b = b\frac{(1+s_d)^{k_d}}{(1+s_p)^{k_p}} \quad (1)$$

$$P_d = d \quad (2)$$

where b and d are the baseline birth and death rates, respectively. Tumor cells are initiated with exactly one driver mutation (i.e. $k_d = 1$) and zero passenger mutations (i.e. $k_p = 0$). During the birth process, cells may undergo mutations at a rate $\mu_d = T_d\mu$ (driver mutations) and $\mu_p = T_p\mu$ (passenger mutations). The model is a spatially-explicit extension of ref.[12] where a driver mutation is a rare event with confers a fitness advantage to birth rate known as s_d and a passenger mutation is relatively common event that confers some fitness penalty, s_p. Here we make the simplifying assumption that each subsequent driver (and each subsequent passenger) has equal effect, rather than a distribution of fitness effects, but others have shown that relaxing this assumption gives similar dynamics[12].

Model parameters

Consistent with the range reported[12,13], the following parameter values were used: $s_d = 0.1$, $s_p = 10^{-3}$, $T_d = 700$, $T_p = 10^6$, $\mu = 10^{-8}$. Due to the possibility of extensive variability in these parameters (see ref.[13]), each of these parameters was varied several orders of magnitude to ensure the robustness of conclusions drawn. Birth and death rates were kept constant at $b = d = 0.5$ unless otherwise noted, and do not significantly alter results for $b, d \in [0.1, 0.5]$ (see figure S1B).

Heterogeneity

Heterogeneity of driver and passenger mutations is calculated using Shannon entropy, given by:

$$H = \exp\left(-\sum_i = p_i \log p_i\right) \quad (3)$$

where p_i is the proportion of cells within the population with exactly i driver (H_d) or passenger (H_p) mutations.

Dispersal rate between glands and ducts

Because there are no reliable data on the probability of tumor cell mixing and dispersal between breast ducts or colon glands, a range of dispersal rates (rate $\in [0.01, 0.1]$) are simulated in dimensions, while realistic breast ductal network structure in three dimensions with varied ductal branch sizes and branching topology (with varied initial conditions) are given by ref.[29].

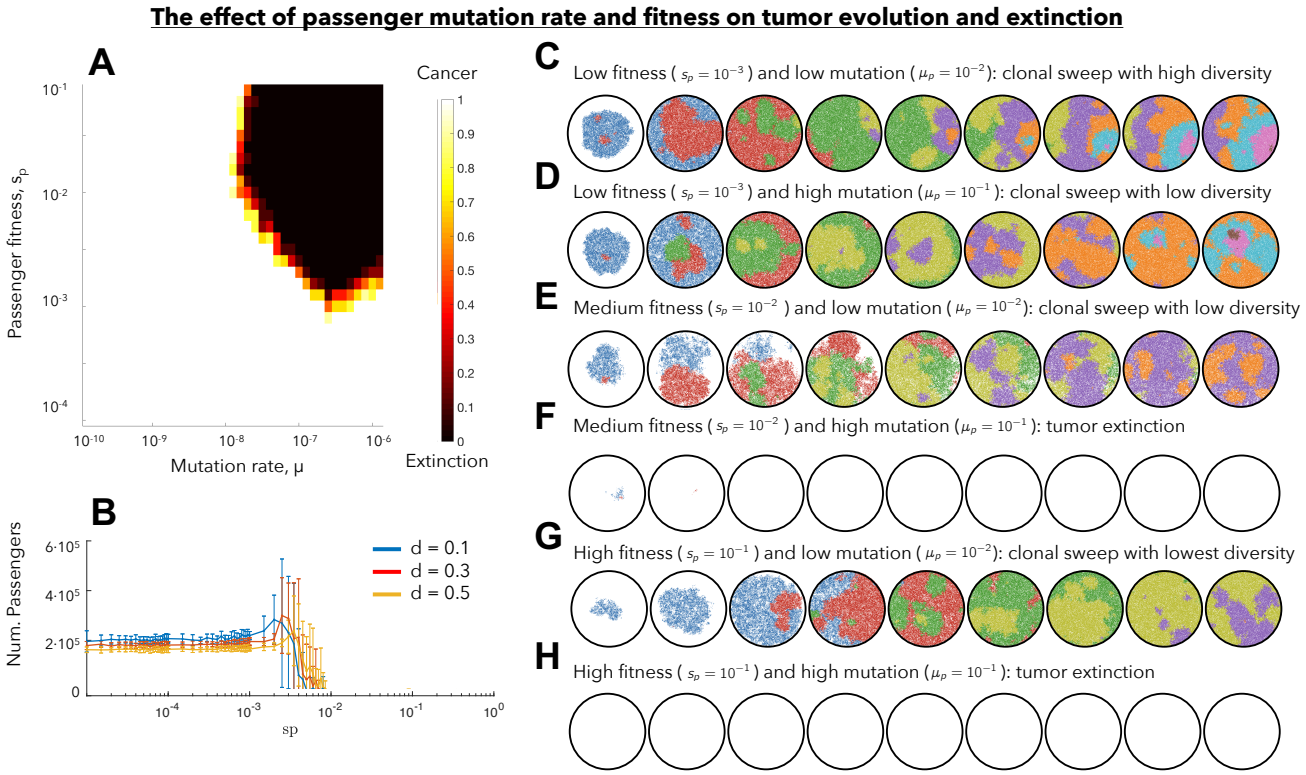

Figure S1. Cancer progression and extinction in passenger driver evolution (A) Rate of cancer progression (simulations that do not go extinct after 10000 cell generations) and extinction depends on passenger fitness penalty, s_p and mutation rate, μ. 10 simulations shown for each parameter value. (B) Low and moderately deleterious passenger mutations can evade negative selection, for a variety of turnover (cell death, d) values. (C) Low passenger fitness penalty and low mutation rate leads to clonal sweep with high diversity at each time point. (D) Low passenger fitness and high mutation rate leads to clonal sweep with lower diversity. (E) Moderate passenger fitness and low mutation rate similarly leads to clonal sweep with lower diversity. (F) Moderate passenger fitness with high mutation rate leads to extinction. (G) High passenger fitness with low mutation rate leads to clonal sweep with lowest diversity. (H) High passenger fitness with high mutation rate leads to tumor extinction.

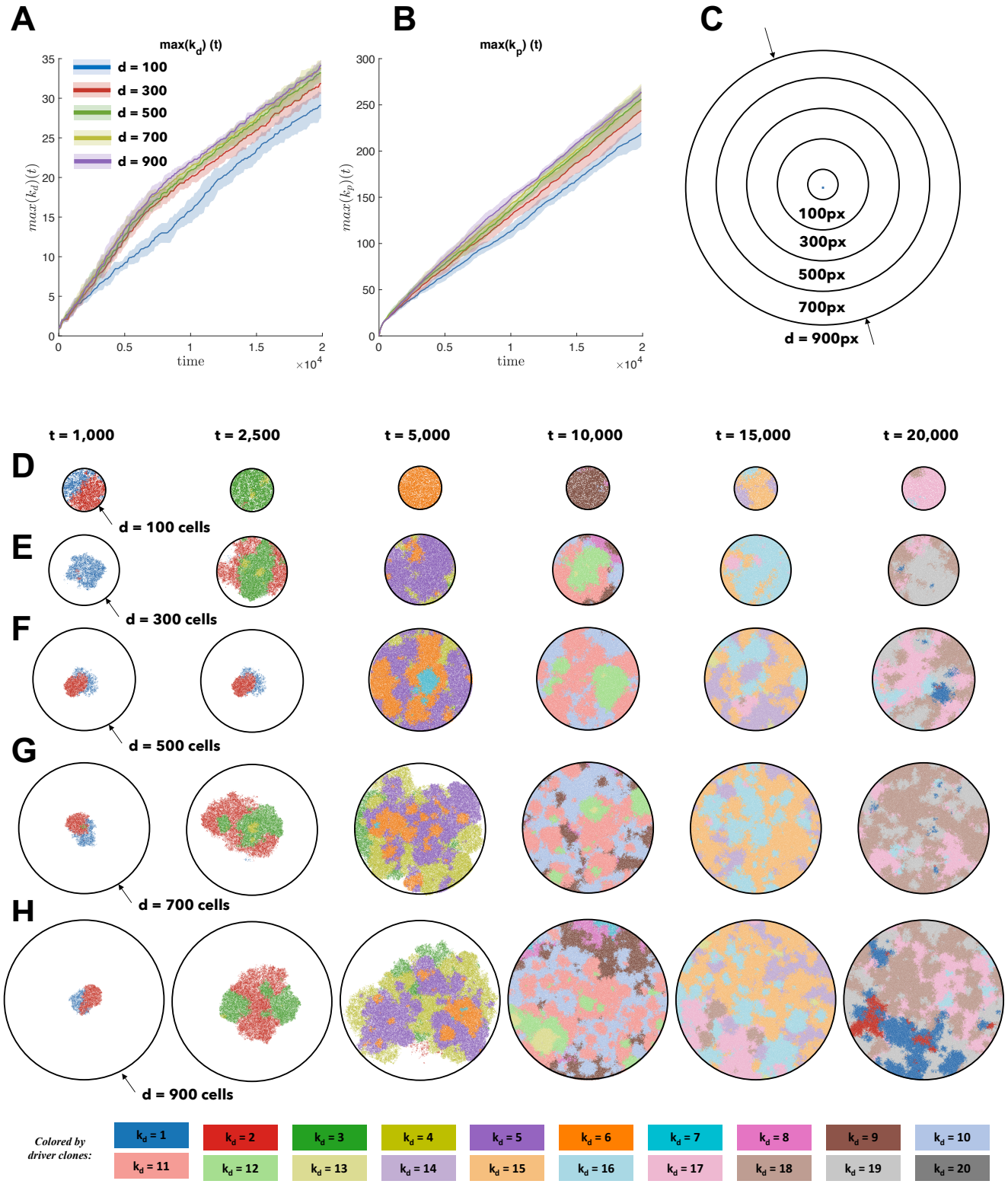

Figure S2. The effect of spatial competition on passenger hitch-hiking The maximum driver number in the population, max(k_d) and the maximum passenger, max(k_p) is shown for a range of size constraints. Apart from the smallest domain size (D) of 100 cells, the maximum driver and passenger for each size constraint are relatively equivalent for each point in time. (C) Domain sizes, shown to scale. (D,E,F,G,H) As seen from the snapshots at each time point the population ranges from heterogeneous (large domains) to homogeneous (smaller domains).

Acknowledgments

The authors gratefully acknowledge funding from the Physical Sciences Oncology Network (PSON) at the National Cancer Institute, U54CA193489 (supporting JW, CG, ARAA). ROS is supported by the Wellcome Trust (grant no. 108861/7/15/7) and the Wellcome Centre for Human Genetics (grant no. 203141/7/16/7). The authors gratefully acknowledge Hanbean Youn for helpful feedback and communication, as well as providing access to data from anthropomorphic breast phantoms used to reconstruct breast ductal networks[29].

Author Contributions

JW and ARAA conceived the research question and model design. JW performed analysis of data from the model and wrote the manuscript with critical comments and input from ARAA and MRT. CG and ROS developed code used to visualize Muller plots and assisted with manuscript edits. All authors have read and edited the final manuscript.